Electrochemistry

The Electrochemical Society of Japan

Received: May 3, 2015
Accepted: October 27, 2015
Published: December 27, 2015

http://dx.doi.org/10.5796/electrochemistry.84.7

Article

Electrochemistry, **84(1)**, 7–11 (2016)

Synthesis of Multiwalled Carbon Nanotube Aqueous Suspension with Surfactant Sodium Dodecylbenzene Sulfonate for Lithium/Sulfur Rechargeable Batteries

Yan ZHAO,[a,b] Xinyi LIU,[a,b] Yongguang ZHANG,[a,b,*] Zhumabay BAKENOV,[c] and Fuxing YIN[a,b,*]

[a] *Research Institute for Energy Equipment Materials, Hebei University of Technology, Tianjin 300130, China*
[b] *Tianjin key laboratory of laminating fabrication and interface control technology for advanced materials, Hebei University of Technology, Tianjin 300130, China*
[c] *Institute of Batteries LLC, Nazarbayev University, Nazarbayev University Research and Innovation System, Kabanbay Batyr Avenue, 53, Astana 010000 Kazakhstan*

* *Corresponding authors: yongguangzhang@hebut.edu.cn, foxing2008@hotmail.co.jp*

ABSTRACT

Due to the hydrophobic nature of multiwalled carbon nanotube (MWNT), sodium dodecylbenzene sulfonate (SDBS) was adopted as a surfactant to synthesize a well-dispersed, homogeneous MWNT aqueous suspension. By simple stirring mixing of the resultant MWNT suspension with nano-sulfur aqueous suspension, a novel porous sulfur/multiwalled carbon nanotube composite (S/MWNT) was synthesized. This preparation method based on the suspension mixing possesses the advantages of simplicity and low cost. Homogeneous dispersion and integration of MWNT in the composite results in a porous, highly conductive and mechanically flexible framework with enhanced electronic conductivity and ability to absorb the polysulfides into its porous structure. The cell with this S/MWNT composite cathode demonstrates a high reversibility, resulting in a stable reversible specific discharge capacity of 708 mAh g^{-1} after 100 cycles at 0.1 C. Furthermore, the S/MWNT composite cathode with sulfur content of 62.5 wt% exhibits a good rate capability with discharge capacities of 946, 780 and 516 mAh g^{-1} at 0.5, 1 and 1.5 C, respectively.

© The Electrochemical Society of Japan, All rights reserved.

Keywords : Carbon Nanotubes, Nanocomposites, Simple Stirring Mixing, Lithium/Sulfur Battery

1. Introduction

Lithium/sulfur batteries have gained intense attention as one of the most promising candidates for high energy density rechargeable batteries due to their high theoretical specific capacity of 1672 mAh g^{-1} and theoretical energy density of 2600 Wh kg^{-1} based on cathode materials.[1] In addition, sulfur has the advantages such as low cost, natural abundance, and environmental friendliness.[2] However, there are still several significant technical limitations that hinder the commercialization of Li/S batteries. The main problems include: low utilization of sulfur because of its poor electrical conductivity and rapid capacity loss on repeated cycling because of dissolution of polysulfides into the electrolytes.[3] Various methods have been explored to address the above mentioned issue, including addition of various types of conductive carbon materials[4–9] and conductive polymers.[10–13] Notably, the dispersion of multiwalled carbon nanotube (MWNT) with sulfur has been proven to be an effective and facile method to reinforce the electric conductivity of the cathode and prevent dissolution of lithium polysulfides into the electrolytes.[4,11]

However, it is known that MWNT has hydrophobic characteristic and cannot be dispersed into sulfur electrode homogeneously, and the cycle performance of a sulfur cathode with simple MWNT addition still remains insufficient for the practical applications.[4] Besides, the reported synthesis methods are usually complicated and challenging for large-scale application.[9]

In this study, we report on the preparation of the long-time stabilized MWNT aqueous suspension with the addition of sodium dodecylbenzene sulfonate (SDBS) surfactant, and a well-dispersed sulfur/multiwalled carbon nanotube (S/MWNT) composite synthesis via a simple stirring mixing of the resultant MWNT suspension with commercial nanosized sulfur aqueous suspension.

2. Experimental

The 0.5 wt% of MWNT and the 0.5 wt% of surfactant SDBS were firstly dispersed into 50 ml of distilled water. Then, the mixture was stirred for 1 h and ultrasonicated for 2 h using a sonicator (Hielscher Ultrasonics). The as-prepared MWNT suspension was separated via filtration, thoroughly washed with deionized water and methanol, and dried in a vacuum oven overnight at 70°C, and a porous structure consisted of MWNT powder (MWNT-*p*) was obtained.

Further, 20 g resulting MWNT suspension was mixed with 3 g aqueous suspension of nano-sulfur (US research nanomaterials Inc, 10 wt%) and stirred for 2 h as schematically presented in Fig. 1. The precipitate was separated via filtration, thoroughly washed with deionized water and methanol, and dried in a vacuum oven overnight at 70°C. Finally, the mixture was heated to 150°C for 3 h in Ar gas atmosphere to obtain the S/MWNT composite. The sulfur content in this composite, determined using chemical analysis (CHNS, Vario Micro Cube, Elementar), was 62.5 wt%. As a control experiment, the S/MWNT mixture was prepared in the same way as the S/MWNT composite but without addition of SDBS.

The crystalline phases of the sample were determined by X-ray diffraction (XRD, D8 Discover, Bruker) equipped with CuKα radiation. The composite surface morphology was examined by field emission scanning electron microscopy (FE-SEM, Leo-1530, Zeiss). The interior structure of sample was observed using transmission electron microscopy (TEM, JEM-2800, JEOL). Nitrogen adsorption

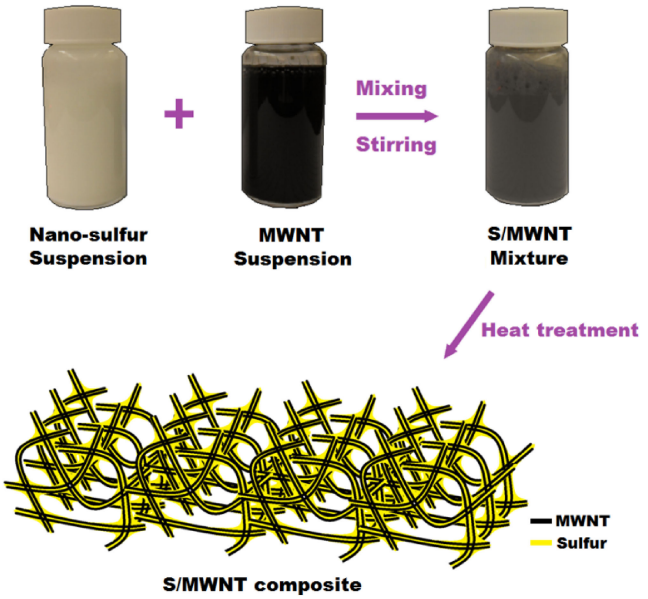

Figure 1. (Color online) Schematics of the S/MWNT composite preparation and a model of the prepared S/MWNT composite structure.

measurements were performed with an autosorb Autosorb iQ instrument (Quantachrome Instruments U.S.) at 77 K. Brunauer-Emmett-Teller (BET) and Barret-Joyner-Halenda (BJH) methods were then used to evaluate the specific surface area and the pore size distribution of the sample.

The electrochemical performance of S/MWNT composite samples was investigated using coin-type cells (CR2025). The cell was composed of lithium metal anode and S/MWNT cathode separated by a microporous polypropylene separator soaked in 1 M lithium trifluoromethanesulfonate ($LiCF_3SO_3$) in dimethoxy ethane (DME) and 1,3-dioxolane (DOL) (1:1 v/v) electrolyte. The composite cathode was prepared by mixing 80 wt% S/MWNT composite, 10 wt% polyvinylidene fluoride (PVDF) (Kynar, HSV900) as a binder and 10 wt% acetylene black (MTI, 99.5% purity) conducting agent in 1-methyl-2-pyrrolidinone (NMP, Sigma-Aldrich, ≥99.5% purity). The resultant slurry was uniformly spread onto aluminum foil using a doctor blade, and dried at 50°C for 12 h. The resulting cathode film was used to prepare the cathodes by punching circular disks with a diameter of 1 cm. The sulfur loading in each electrode was about 3 mg cm^{-2}. The S/MWNT mixture cathode, with a weight ratio S/MWNT mixture:AB:PVdF = 8:1:1 was prepared in the same way as the S/MWNT composite cathode. The coin cells were assembled in an Ar (99.9995%) filled glove box (MBraun) and tested galvanostatically on a multichannel battery tester (BTS-5V5mA, Neware) between 1 and 3 V vs. Li^+/Li electrode at different current densities. Cyclic voltammetry (CV) was performed with a potentiostat (VMP3, Biologic) between 1 and 3 V vs. Li^+/Li at a scanning rate of 0.5 mV s^{-1}. Applied currents and specific capacities were calculated on the basis of the weight of S in each cathode. Electrochemical impedance spectroscopy (EIS) was measured by using the same electrochemical workstation within a frequency range from 0.01 to 100 kHz.

3. Results and Discussion

Figure 2 shows the XRD patterns of the as-prepared S/MWNT composite, sulfur and MWNT. The JCPDS card data of sulfur (PDF reference number 01-083-2284) are also shown in the figure. It can be seen from the XRD patterns that for the S/MWNT composite, the characteristic peaks of crystal sulfur are present but with a reduced intensity and broad peak around 26°. This is most likely

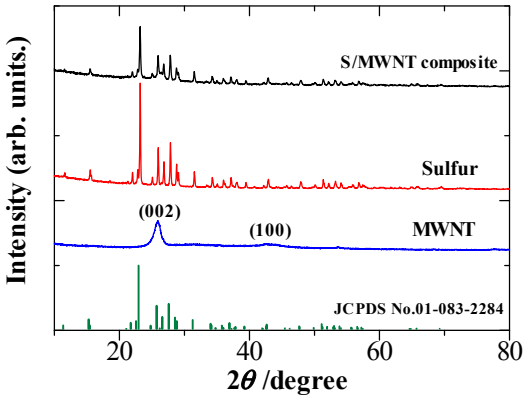

Figure 2. (Color online) XRD patterns of sulfur, MWNT, S/MWNT composite and JCPDS 01-083-2284: sulfur.

consequence of the well-dispersed character of nanoscopic sulfur in the composite, as evidenced by the following EDS analysis.

The surface morphology and structure of the MWNT-*p* were imaged by TEM and SEM and presented in Fig. 3a and 3b, respectively. It can be seen that MWNT irregularly stacks together, forming a highly porous structure. This porous MWNT network could serve as not only a 3D interlinked current collector for long range electron transfer but also as a macroporous robust matrix to allow deep penetration of the electrolyte and to prevent segregation of sulfur particles.[14] Figure 3c and 3d present the SEM images of S/MWNT mixture at different magnification. One can see that the S/MWNT mixture is highly agglomerated. In contrast, the SEM images of the S/MWNT nanocomposite in Fig. 3e and 3f at low and high magnifications show that S particles are well embedded into MWNT. Sulfur and MWNT form a uniformly distributed hybrid material with a well-dispersed three-dimensional network structure. This is in good agreement with the EDS mapping (Fig. 3g–3i), confirming the homogeneous dispersion of S and MWNT in the S/MWNT nanocomposite. On the other hand, the EDS mapping of S/MWNT mixture (Fig. 3j–3l) shows less homogeneous and distribution of sulfur and carbon in this system, exhibiting agglomerated and poor dispersion. This could be due to a lower degree of mixing of MWNT with sulfur without addition of SDBS, which, consequently, might negatively affect the electrochemical performance of this mixture due to poor conductivity between sulfur particles isolated from conductive MWNT network. In contrast, enhanced distribution of sulfur in a conductive network/mesh of MWNT in the S/MWNT composite favors conductivity between the sulfur particles, which improves sulfur utilization as a cathode active material, and can effectively hold the electrochemical reaction products, polysulfides.

In order to confirm the highly porous structure of S/MWNT composite, the BET measurements were conducted. As shown in Fig. 4, a characteristic type I isotherm is observed. The total pore volume of the S/MWNT composite is measured to be 0.57 cm^3 g^{-1}, and the BET surface area is about 93 m^2 g^{-1}, whereas the BET surface area of S/MWNT mixture prepared without adding SDBS is only 9.6 m^2 g^{-1} with the pore volume of 0.05 cm^3 g^{-1}. This remarkable difference of specific surface area and pore volume could be attributed to the highly porous structure formed in the S/MWNT composite, which can supply more electrochemical reaction sites and act as pathways for the electrolyte diffusion.[15] Furthermore, in the S/MWNT composite, the BET surface area of 63 m^2 g^{-1} comes from the micropores' contribution, exhibiting the abundance of micropores, which is efficient to restrict the polysulfides diffusion during the charge/discharge process.

The CV curves of the S/MWNT composite cathode active material in the lithium half-cell are shown in Fig. 5. One can see that two reduction peaks around 2.3 and 2.0 V vs. Li^+/Li and one

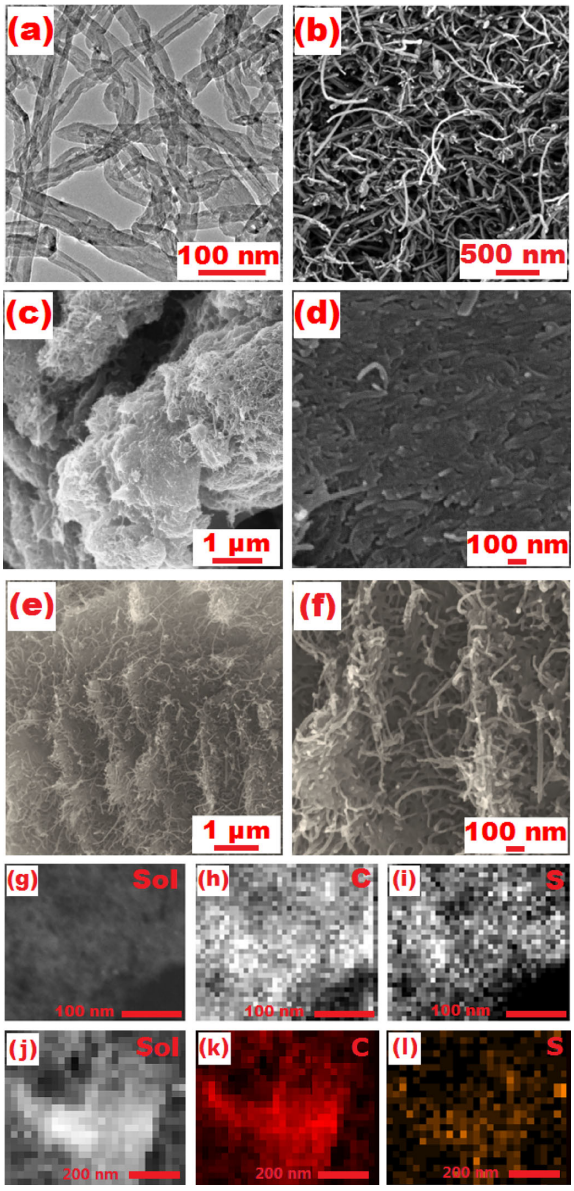

Figure 3. (Color online) (a and b) TEM and SEM images of MWNT-*p*; (c and d) SEM images of S/MWNT mixture at different magnification; (e and f) SEM images of S/MWNT composite at different magnification; (g) TEM image and elemental mapping of carbon (h) and sulfur (i) by energy-dispersive X-ray spectroscopy (EDS) of S/MWNT composite; (j) TEM image and elemental mapping of carbon (k) and sulfur (l) by energy-dispersive X-ray spectroscopy (EDS) of S/MWNT mixture.

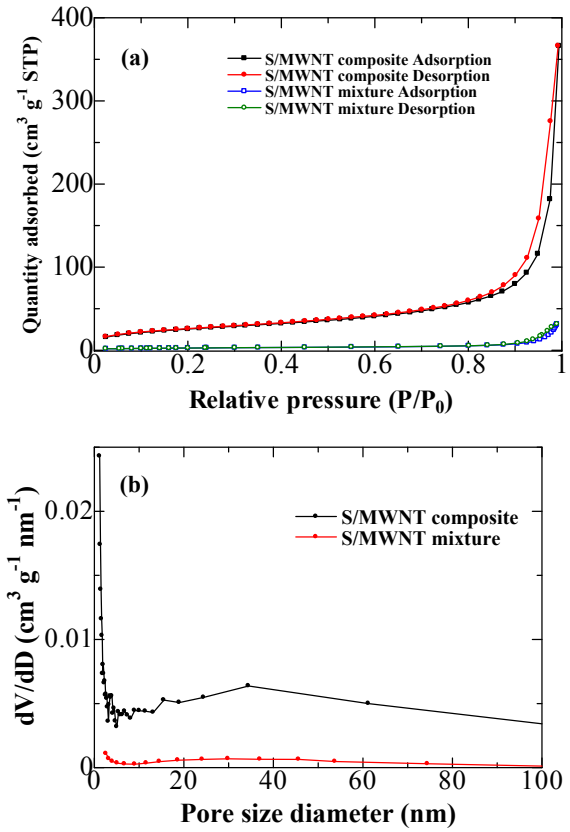

Figure 4. (Color online) (a) Nitrogen adsorption/desorption isotherms and (b) pore size distributions of the S/MWNT composite and S/MWNT mixture.

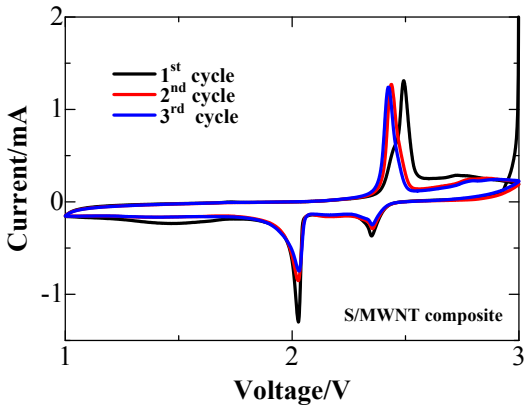

Figure 5. (Color online) Initial CV profiles of S/MWNT composite (a potential sweep rate is 0.5 mV s^{-1}).

oxidation peak around 2.5 V are observed in the S/MWNT composite in the first cycle. The reduction peak at 2.3 V corresponds to the conversion of the elemental sulfur to the lithium polysulfides (Li_2S_n, $n \geq 4$). Another reduction peak clearly identified at 2.0 V during the first cathodic scan can be attributed to the deep reduction of polysulfides into insoluble Li_2S_2/Li_2S. The oxidation peak at 2.5 V is associated with the reversible transformation of Li_2S_2/Li_2S into the polysulfides.[6]

The initial profiles of galvanostatic charge/discharge tests of the S/MWNT cathode are shown in Fig. 6. It can be seen that two main plateaus appear in the potential profiles, which could be attributed to two main electrochemical processes taking place at the sulfur cathode upon cycling in Li/S battery. The results are in good agreement with the CV data. The S/MWNT nanocomposite delivers a high initial discharge capacity of about 1394 mAh g^{-1} at 0.1 C.

The enhanced polysulfide trapping capability of the S/MWNT composite is reflected in the cycle performance. As shown in Fig. 7, both the S/MWNT composite and S/MWNT mixture deliver high initial capacities of 1394 and 1241 mAh g^{-1} at 0.1 C, respectively. Upon cycling, the discharge capacity of the S/MWNT mixture drastically decreases and maintains only 507 mAh g^{-1} after 100 cycles. In comparison with the S/MWNT mixture cathode, the S/MWNT composite counterpart exhibits a remarkably enhanced performance. After two initial cycles, the porous S/MWNT composite electrode displays a discharge capacity of 993 mAh g^{-1} at 0.1 C, and maintains a capacity of more than 700 mAh g^{-1} after 100 cycles. The sulfur shuttle mechanism is a typical phenomenon in lithium/sulfur batteries, resulting in imperfect charging and

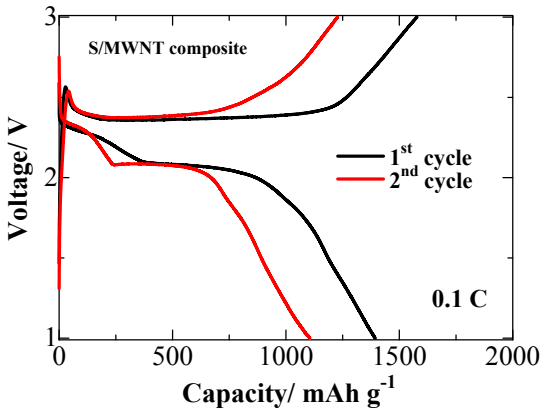

Figure 6. (Color online) The initial discharge/charge profiles of a lithium cell with S/MWNT composite cathode at 0.1 C.

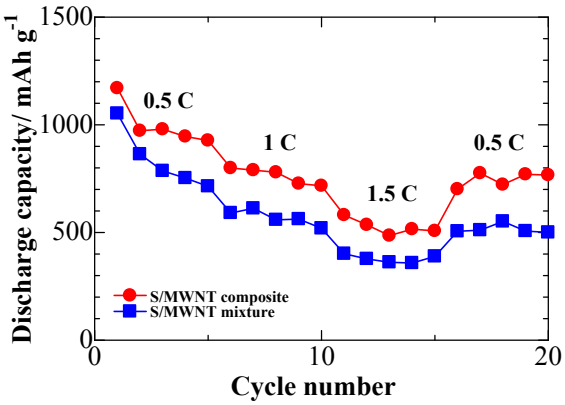

Figure 8. (Color online) Rate capability of lithium cells with the S/MWNT composite and S/MWNT mixture cathodes.

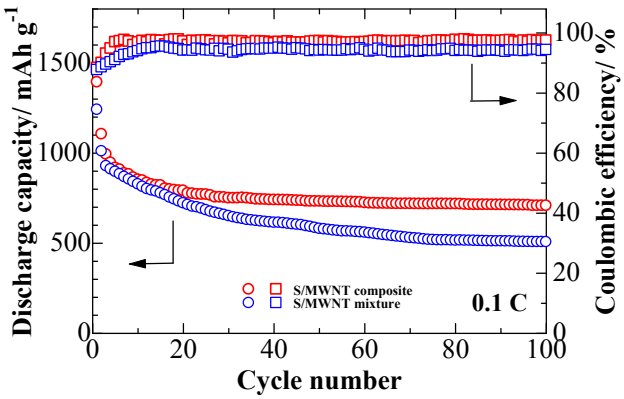

Figure 7. (Color online) Cycle performance of lithium cells with S/MWNT composite and S/MWNT mixture cathodes at 0.1 C.

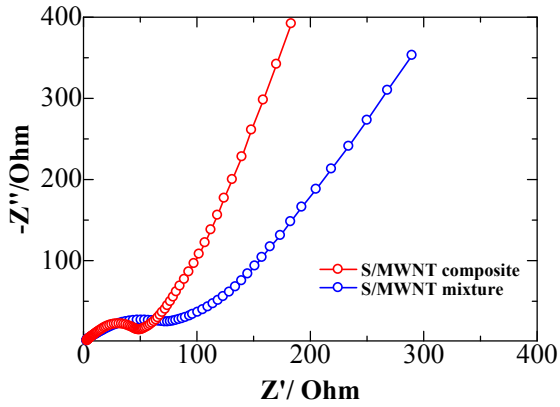

Figure 9. (Color online) Nyquist plots of the S/MWNT composite and S/MWNT mixture cathodes after the first charge/discharge cycle.

decreasing its discharge capacity, which leads to a low coulombic efficiency of the cell.[16] Fig. 7 presents the cell coulombic efficiency vs. cycle number for both the S/MWNT composite and S/MWNT mixture cathodes. The S/MWNT composite maintains a high coulombic efficiency in a range of 88.3–97.8%, showing an improved coulombic efficiency compared with the S/MWNT mixture. This suggests that the homogeneous dispersion of MWNT in S/MWNT composite, which was achieved by addition of a surfactant (SDBS) into the precursor suspension, not only provides a stable electron conduction path for the sulfur electrode, but also restricts the polysulfides diffusion during the charge/discharge process.

The comparative data on rate capability properties of the S/MWNT composite and the S/MWNT mixture are presented in Fig. 8. With the increase in the current rate from 0.5 C to 1.5 C, the discharge capacity of the S/MWNT composite drops from about 946 mAh g^{-1} to 516 mAh g^{-1}. For this composite, the discharge capacity could be mostly recovered when the current density is decreased back from 1.5 C to 0.5 C, showing a great advantages of the S/MWNT nanocomposite for the abuse tolerance under different current densities. In contrast, the discharge capacity of the S/MWNT mixture decreased sharply with the C rate increase, and its discharge capacity is only partly recovered (70%) when the cycling rate is switched back to 0.5 C. It could be suggested that the introduction of homogeneously-dispersed MWNT suspension as precursor to prepare S/MWNT composite is an effective way to improve the cathodes rate capability by enhancing the charge transfer properties. This suggestion has been confirmed by the following EIS studies.

EIS is a powerful tool to study the charge transfer behavior in the composite cathode materials. The comparative EIS data for the S/MWNT composite and S/MWNT mixture measured after the initial charge/discharge cycle are shown in Fig. 9. It can be seen that for both cathodes the Nyquist plots are presented by a semicircle in the high-to-medium frequency range, related to interfacial charge transfer impedance, followed by a declined line of the Warburg impedance in the low frequency part attributed to the bulk diffusion resistance of the composite cathode.[17,18] A much smaller high-to-medium frequency semicircle can be seen in the S/MWNT composite electrode EIS spectra compared with that of the S/MWNT mixture. These trends support our suggestion on the conducting property enhancement by addition of a homogeneously-dispersed MWNT suspension as precursor to prepare S/MWNT composite.

4. Conclusions

A simple method for fabricating a homogeneous and well-dispersed S/MWNT composite has been developed. The method, which employs commercial nanosized sulfur particle suspension and MWNT suspension, guarantees homogeneous dispersion of S and MWNT in the composite. In this work, we adopted sodium dodecylbenzene sulfonate as a surfactant to prepare a well-dispersed, homogeneous MWNT aqueous suspension. From SEM, TEM and the EDS mapping results, it was confirmed that a uniformly distributed hybrid material with a porous network structure was successfully synthesized. As-synthesized S/MWNT composite has been tested as a cathode in rechargeable Li/S

batteries. The S/MWNT composite exhibits excellent performance with a high initial capacity up to 1394 mAh g^{-1} and a stabilized capacity of 708 mAh g^{-1} after 100 cycles at 0.1 C, which could be attributed to the uniform dispersion of sulfur with MWNT enabled by the simple suspension mixing synthesis method and resulting charge transfer impedance reduction.

Acknowledgments

The authors are grateful of financial support by the National Natural Science Foundation of China (Grant No. 21406052), financial support by the Program for the Outstanding Young Talents of Hebei Province (Grant No. BJ2014010); ZB acknowledges the Sub-project #157-2013 funded under the Technology Commercialization Project by the World Bank and the Government of the Republic of Kazakhstan.

References

1. A. Manthiram, Y. Z. Fu, and Y. S. Su, *Acc. Chem. Res.*, **46**, 1125 (2013).
2. X. L. Jia and L. F. Nazar, *J. Mater. Chem.*, **20**, 9821 (2010).
3. Y. Zhang, Y. Zhao, K. E. K. Sun, and P. Chen, *Open Mater. Sci. J.*, **5**, 215 (2011).
4. L. X. Yuan, H. P. Yuan, X. P. Qiu, L. Q. Chen, and W. T. Zhu, *J. Power Sources*, **189**, 1141 (2009).
5. L. Zhu, H. J. Peng, J. Y. Liang, J. Q. Huang, C. M. Chen, X. F. Guo, W. C. Zhu, L. Lie, and Q. Zhang, *Nano Energy*, **11**, 746 (2015).
6. Z. J. Sun, M. Xiao, S. J. Wang, D. M. Han, S. Q. Song, G. H. Chen, and Y. Z. Meng, *J. Power Sources*, **285**, 478 (2015).
7. Y. Zhao, Y. Zhang, Z. Bakenov, and P. Chen, *Solid State Ionics*, **234**, 40 (2013).
8. Y. Zhang, Y. Zhao, and Z. Bakenov, *Ionics*, **20**, 1047 (2014).
9. S. Evers and L. F. Nazar, *Chem. Commun.*, **48**, 1233 (2012).
10. Y. S. Su and A. Manthiram, *J. Power Sources*, **270**, 101 (2014).
11. Y. Zhang, Y. Zhao, Z. Bakenov, M. Tuiyebayeva, A. Konarov, and P. Chen, *Electrochim. Acta*, **143**, 49 (2014).
12. X. W. Wang, Z. A. Zhang, X. L. Yan, Y. H. Qu, Y. Q. Lai, and J. Li, *Electrochim. Acta*, **155**, 54 (2015).
13. L. Duan, J. C. Lu, W. Y. Liu, P. Huang, W. S. Wang, and Z. C. Liu, *Colloids Surf., A*, **414**, 98 (2012).
14. L. Zhu, H. J. Peng, J. Liang, J. Q. Huang, C. M. Chen, X. Guo, W. Zhu, P. Li, and Q. Zhang, *Nano Energy*, **11**, 746 (2015).
15. Y. Qu, Z. Zhang, X. Zhang, G. Ren, X. Wang, Y. Lai, Y. Liu, and J. Li, *Electrochim. Acta*, **137**, 439 (2014).
16. Y. Zhang, Y. Zhao, A. Konarov, Z. Li, and P. Chen, *J. Alloys Compd.*, **619**, 298 (2015).
17. Z. Bakenov and I. Taniguchi, *J. Electrochem. Soc.*, **157**, A430 (2010).
18. Y. Zhang, Y. Zhao, Z. Bakenov, M. R. Babaa, A. Konarov, C. Ding, and P. Chen, *J. Electrochem. Soc.*, **160**, A1194 (2013).